Letters

An Electrical Model of a Dielectric Elastomer Generator

Ramanuja Panigrahi and Santanu K. Mishra

***Abstract*—Elastomer is an electroactive polymer, which finds popular application in the field of actuators and artificial muscles. Though elastomers are popularly used as actuators, with proper modification to their operating cycle, they can also be used as generators. These dielectric elastomer generators (DEGs), due to properties such as high energy density and frequency independent operation are suitable for different energy harvesting applications. In this letter, a simplified electrical model of the DEG is proposed, which can be used in various simulation platforms to verify compatibility of DEG with electrical circuits and predict its behavior. Detailed process of deriving the model parameters from a physical DEG is discussed at length. Performance of the proposed model is verified by comparing its behavior with a prototype DEG-based energy harvesting system having a DEG of 1.3 nF capacitance. The proposed DEG model was simulated with similar conditions and the simulation results have shown good accuracy with the experimental results.**

***Index Terms*—Capacitors, circuit modeling energy harvesting, circuit simulation, generators, modeling.**

I. Introduction

ELASTOMER or elastic polymer is a special dielectric material which changes its dimensions under the influence of electric field [1]. Due to this electroactive property, elastomers are popularly used as actuators, active vibration controllers, speakers, gaskets, grippers, artificial muscles, etc. [2]–[4]. Due to numerous advantages of elastomer actuators [1]–[4], their potential to act as generators is being investigated [5]. This gives rise to operation of elastomer as generators, known as dielectric elastomer generator (DEG). As listed in Table I, DEG possesses much higher energy density of 400 mJ/cm^3, compared to competing electromechanical generator technologies. Apart from superior energy density, properties such as inherent amplification, large change in capacitance, frequency independent operation, high dielectric breakdown strength, etc., make DEG an interesting option for different energy harvesting applications [1], [5]. DEG can be used to harvest electrical energy from environmental mechanical vibrations such as human movement, building vibrations, waves, etc.

TABLE I
Comparison of Energy Conversion Technologies [5], [6]

Energy Harvesting Method	Energy Density (mJ/cm^3)	
	Maximum Theoretical	Maximum Achieved
Dielectric elastomer generator	1500	400
Piezoelectric	335	17.7
Electromagnetic	400	4
Conventional variable capacitor generator	44	4

Modeling of DEG is the process of making DEG easier to understand, visualize, and simulate in various computational platforms. DEG model can be used to check compatibility of different electronic circuits with DEG without making a physical DEG. A mathematical simulation model for DEG is proposed in [7], which presents a nonlinear model of a DEG considering biaxial stretch mode. An emulator to imitate DEG behavior is introduced in [8]. In [9] and [10], the electrostatic and mechanical properties of the elastomer actuator are represented in the form of equations separately and are later combined to give the complete model. DEG is represented by an electromechanical Neo-Hooken's model in [11]. A model to predict the maximum energy density limit for a diamond-shaped DEG is proposed in [12]. In [13] a numerical multiphysics model of an electret–elastomer combination is introduced. Thus, the attempts to model a DEG, previously, are mostly limited to mathematical modeling only [7]–[13]. In this letter, a circuit model for DEG is proposed, which represents the DEG as a combination of different electrical components.

This letter is organized as follows. Theory of DEG is introduced in Section II. The proposed model along with its parameters is introduced in Section III. The process of obtaining model parameters from a physical DEG is discussed in Section IV. The model is verified by comparing its performance with an actual DEG, and the results obtained are presented in Section V. Section VI concludes the letter.

II. DEG Fundamentals

A. Construction of DEG

For this realization, elastomer material (3M-VHB 4910) is prestretched three times biaxially and attached to a rigid circular

Manuscript received June 19, 2017; revised August 5, 2017; accepted August 22, 2017. Date of publication September 5, 2017; date of current version January 3, 2018. *(Corresponding author: Ramanuja Panigrahi.)*

The authors are with the Department of Electrical Engineering, Indian Institute of Technology, Kanpur 208016, India (e-mail: ramanuja@iitk.ac.in; santanum@iitk.ac.in).

Color versions of one or more of the figures in this letter are available online at http://ieeexplore.ieee.org.

Digital Object Identifier 10.1109/TPEL.2017.2749329

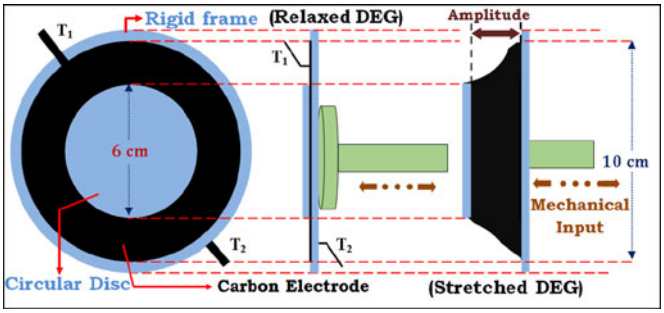

Fig. 1. Front view and side view of a physical DEG.

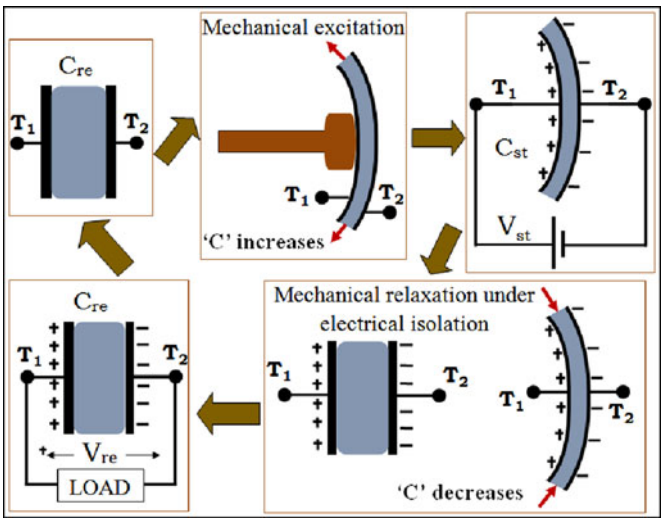

Fig. 2. DEG energy harvesting cycle.

ring of 10 cm diameter. Pre-stretching is necessary to improve response speed and electromechanical stability of elastomer film [2]. A circular disc of 6 cm diameter is adhered to the center of the elastomer to act as the point of application of mechanical vibration. To form adaptable electrodes, both sides of this elastomer film are painted with carbon grease. Fig. 1 shows the front view and the side view of a physical DEG. A parallel plate capacitor is formed between these carbon electrodes (T_1 and T_2) with elastomer as the dielectric.

B. DEG Energy Harvesting Cycle

DEG energy harvesting cycle is based on electrostatic energy conversion principle and can be explained as a series of five steps [14], as shown in Fig. 2.

1) Capacitance of the parallel plate capacitor, formed between electrodes (T_1 and T_2) of DEG, depends on electrode area (A) and thickness of the elastomer film (d) obeying $C \alpha A/d$. Let the capacitance of DEG, in relaxed condition, be C_{re}.
2) Biaxial mechanical stress is applied to DEG, causing the electrode area to increase and thickness of the elastomer to reduce. As a result, the capacitance of DEG increases to C_{st}.
3) In this stretched condition, the electrical supply (V_{st}) is connected between the DEG terminals (T_1, T_2). Due to this priming, charge $Q_{st}(= C_{st}\ V_{st})$ is stored in the DEG and energy $E_i = 0.5 C_{st} V_{st}^2$ is transferred to the DEG.
4) The applied mechanical stress is removed while maintaining electrical isolation. Charge held in relaxed DEG is given by $Q_{re} = C_{re}\ V_{re}$. As DEG is relaxed under electrical isolation, the net charge stored in the DEG remains constant, i.e.

$$Q_{st} = Q_{re} \quad \text{or} \quad C_{st}\ V_{st} = C_{re}\ V_{re}.$$

Simplifying the aforementioned condition, DEG voltage gain (K) can be obtained

$$K = \frac{V_{re}}{V_{st}} = \frac{C_{st}}{C_{re}}. \tag{1}$$

C_{st} depends on the amplitude of applied mechanical vibration, and so does K. As $C_{st} > C_{re}$, K is always greater than 1.

5) The relaxed DEG is connected to a load to deliver the harvested energy. Energy transferred from DEG to load is given by $E_f = 0.5 C_{re} V_{re}^2$. After complete discharge, DEG returns to its typical relaxed, uncharged condition, completing the energy harvesting cycle. The amount of energy harvested in one cycle of DEG operation is given by

$$E = 0.5 C_{re} V_{re}^2 - 0.5 C_{st}\ V_{st}^2 = 0.5 C_{st} V_{st}^2\ (K - 1). \tag{2}$$

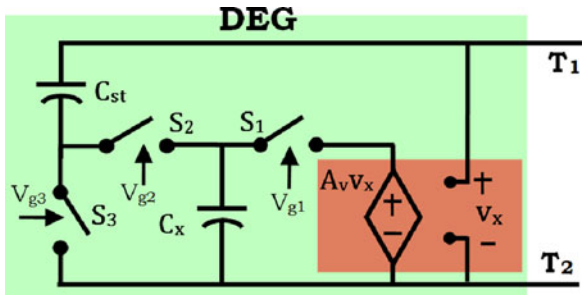

Fig. 3. Proposed DEG circuit model.

III. Proposed Model

From the DEG energy harvesting cycle it is worth noting that:

1) Capacitance of the relaxed DEG (C_{re}) is fixed once the DEG is constructed. But capacitance of the stretched DEG depends on both C_{re} and the amplitude of the mechanical stress.
2) DEG is connected to source only when it's stretched and connected to load only when it's relaxed.
3) When connected to source, DEG behaves as a capacitances C_{st} between terminals T_1 and T_2 and when connected to load DEG acts as capacitance C_{re}. When DEG is being stretched or relaxed, it operates in electrical isolation.

The DEG model must reflect these electromechanical dependencies. The proposed circuit model of DEG is shown in Fig. 3. The model consists of two capacitors (C_{st}, C_x), three controlled switches ($S_1 - S_3$), and one voltage-controlled voltage source

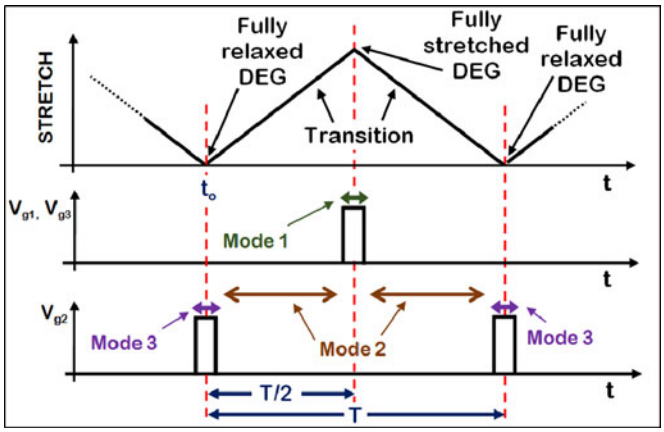

Fig. 4. Timing diagram mapping operation of physical DEG to the model.

(VCVS). The proposed model requires two types of inputs from the user:

1) Control inputs (for $S_1 - S_3$): Map the frequency of mechanical vibration to model.
2) Parametric Inputs (C_{st}, C_x, A_v): Depend on the construction of DEG and amplitude of the applied mechanical vibration.

A. Derivation of Control Input

Fig. 4 is used to map DEG physical operating time to the model switching. In one operating cycle, as explained in Section-II, DEG is subjected to maximum stretch and returns back to relaxed condition. The DEG is connected to external electrical system only when it is fully stretched or fully relaxed. To ensure similar behavior of the model, control signal to the switches S_1 and S_3 is high when DEG is fully stretched and control signal for the switch S_2 is high only when DEG is fully relaxed. At $t = t_0$, to replicate relaxed DEG, S_2 is turned on and the model operates in Mode 3. At $t = t_0 + T/2$, DEG is fully stretched. To imitate this, S_1 and S_3 are turned on and the model operates in Mode 1. At $t = t_0 + T$, the cycle completes and DEG returns to its relaxed condition. The time period "*T*" is reciprocal of the frequency (*f*) of mechanical vibration. During the transition from Mode 3 to Mode 1 and vice versa, the model operates in Mode 2. All these modes are investigated further and are depicted in Fig. 5.

B. Parameter Selection

To derive the parametric inputs, behavior of the model in different modes is examined. Depending on the state of the control signals, the proposed model operates in three different modes.

Mode 1: When the DEG is fully stretched, it is connected to V_{st} and the capacitance seen between terminals T_1 and T_2 is C_{st}. In model, this is achieved by turning switch S_1 and S_3 on, as shown in Fig. 5(a). As S_3 is on, capacitor C_{st} is connected between terminals T_1 and T_2. Capacitor C_x is charged by the VCVS through S_1. As ideal VCVS is used, it takes no energy from the supply (V_{st}). This mode represents step 3 of DEG energy harvesting cycle.

Mode 2: During the process of stretching or relaxing, physical DEG is in complete electrical isolation. To achieve this in the model, all switches are kept off. This mode, depicted in Fig. 5(b), is an alias of the DEG condition during steps 2 and 4 of the energy harvesting cycle.

Mode 3: The relaxed DEG is connected to load and the capacitance seen between T_1 and T_2 is C_{re}.This condition is replicated in the model by turning S_2 on, as shown in Fig. 5(c). The model in Mode 3 represents steps 1 and 5 of the energy harvesting cycle.

To imitate DEG energy harvesting cycle, the model traverse through Mode 3–Mode 2–Mode 1–Mode 2–Mode 3 of its operation. In Mode 1, the capacitance of the model must be equal to that of stretched DEG. So capacitor C_{st} is used directly in the model. In Mode 3, equivalent capacitance offered by the model, between T_1 and T_2, must be equal to C_{re}. As C_{st} and C_x are in series during Mode 3, value of C_x can be evaluated by equating their series equivalent capacitance to C_{re}

$$\frac{C_{st} \times C_x}{C_{st} + C_x} = C_{re}.$$

Substituting the value of C_{re} from (1) and solving, we get

$$C_x = \frac{C_{st}}{K - 1}. \tag{3}$$

Voltage gain to be produced by the DEG model, while shifting from Mode 1 to Mode 3, is "*K*." C_{st} and C_x are in series, and C_{st} is at a potential V_{st}. So to get an effective gain of "K," gain (A_v) of VCVS is fixed at $K - 1$

$$A_v = K - 1. \tag{4}$$

From (3) and (4), it is clear that, in order to determine the value of model parameters, C_{st} and *K* of the physical DEG must be measured.

The energy harvested in physical DEG comes from mechanical vibrations and is equal to *E* given in (2). In the proposed model, this energy (E_v) is provided by the VCVS and is given by

$$E_v = 0.5 \times C_x \times [A_v \times V_{st}]^2. \tag{5}$$

Replacing C_x and A_v in (5) from (3) and (4), respectively, we get

$$E_v = 0.5 C_{st} V_{st}^2 (K - 1). \tag{6}$$

From (2) and (6), it is evident that energy supplied by the VCVS is identical to the amount of energy harvested from mechanical vibration by the physical DEG.

IV. Determination of Model Parameters from a Physical DEG

A. Determination of C_{st}

For the measurement of C_{st}, stretched DEG is connected to a dc voltage source and oscilloscope through a mechanical Single pole double throw (SPDT) switch as

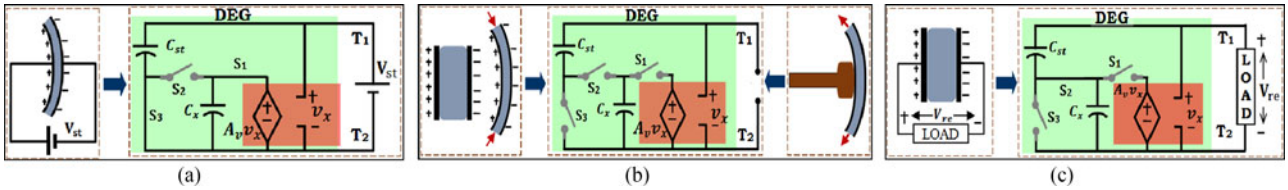

Fig. 5. State of DEG model in different Modes of operation. (a) Mode 1, (b) Mode 2, and (c) Mode 3.

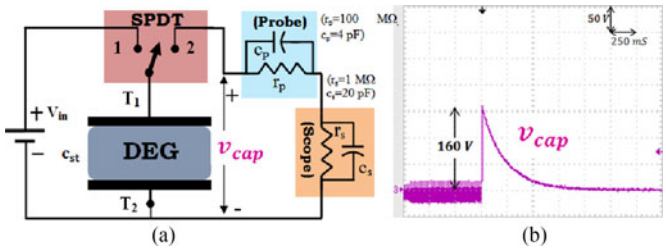

Fig. 6. Experimental setup used to measure C_{st}. (a) Schematic diagram and (b) voltage measured by the oscilloscope.

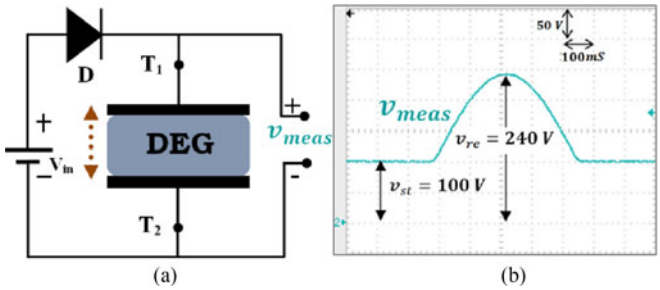

Fig. 7. Experimental setup used to measure *K*. (a) Schematic diagram and (b) voltage measured during stretching and relaxing of DEG.

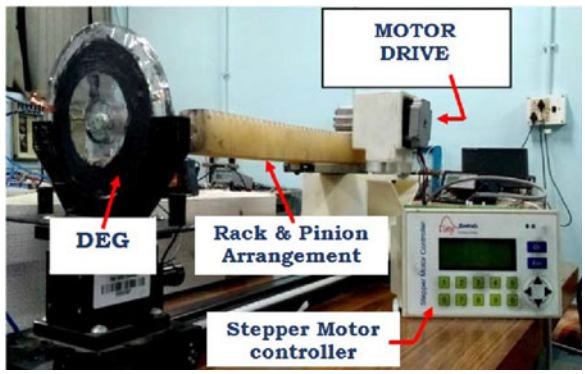

Fig. 8. Experimental setup of the DEG and associated mechanical exciter.

shown in Fig. 6(a). Initially, SPDT is connected to 1 so that DEG gets charged to V_{in}. SPDT is then moved to position 2. DEG discharges through the oscilloscope and voltage across the DEG is recorded.

The behavior of the circuit, when SPDT is placed at 2, can be explained by a second order differential equation as follows.

$$a_1 \frac{d^2 v_{\text{cap}}}{dt^2} + a_2 \frac{dv_{\text{cap}}}{dt} + a_3\, v_{\text{cap}} = 0 \tag{7}$$

where $a_1 = r_s\ (c_{st}c_p + c_{st}c_s + c_p c_s)$, $a_2 = c_{st}\ r_p + c_{st} r_s + c_s r_s + c_p r_p$, and $a_3 = 1$

Mathematically obtained solution of (7) predicts that the effect of scope resistance (r_s) and scope and probe parasitic capacitance (c_s and c_p, respectively) on voltage discharge profile is negligible. Thus, the effective loading of both probe and scope can be emulated as a simple resistor (R_{eff}) having resistance equal to r_p

$$R_{\text{eff}} = r_p\ .$$

Time constant (τ) of this source-free *RC* circuit is given by

$$\tau\ = C_{st}\ \times R_{\text{eff}}. \tag{8}$$

The experimentally obtained DEG voltage discharge profile is shown in Fig. 6(b). Time constant of this voltage discharge profile is 310 ms. The equivalent loading (R_{eff}) is equal to 100 MΩ for Tektronix P-5122 probe. By replacing τ and R_{eff} in (8), C_{st} is evaluated and is found to be 3.1 nF.

B. Determination of K

An experimental arrangement, to measure DEG voltage gain *K*, is shown in Fig. 7(a). DEG, connected in the system, is stretched and relaxed, continuously. During stretching, diode *D* conducts and DEG gets charged to the input voltage V_{in}, i.e., $V_{st} = V_{\text{in}}$. With relaxation of DEG, voltage across terminals T_1 and T_2 increases beyond V_{in} keeping the diode (*D*) reverse biased. Maximum voltage (V_{re}) occurs across $T_1 - T_2$ when the DEG is fully relaxed. Variation in DEG voltage during one cycle is shown in Fig. 7(b). Voltage gain *K* of the DEG is evaluated using (1), i.e., V_{re}/V_{st}, and is found to be 2.4.

Once C_{st} and K are known, all model parameters can be found out by using (3) and (4).

V. Model Verification

To verify the effectiveness of the proposed model, its behavior is compared with a physical DEG. Prototype of a DEG-based energy harvesting system is designed in laboratory. A schematic of the same system, where DEG is replaced by the proposed model, is simulated in PSpice simulation platform. The physical DEG system is divided into mechanical and electrical subsystems.

A. Mechanical Subsystem

The mechanical subsystem, shown in Fig. 8, consists of a DEG and a mechanical exciter. A stepper motor drive along with a Rack and pinion arrangement is used to replicate the environmental vibration and acts as the mechanical exciter.

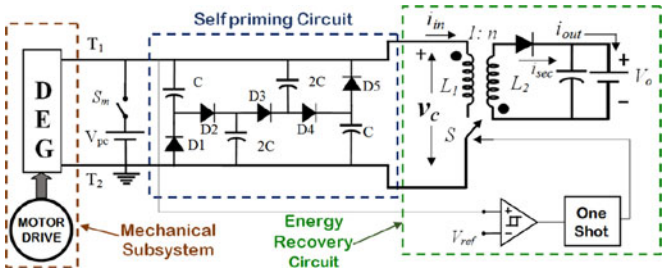

Fig. 9. Complete electrical system driving the DEG.

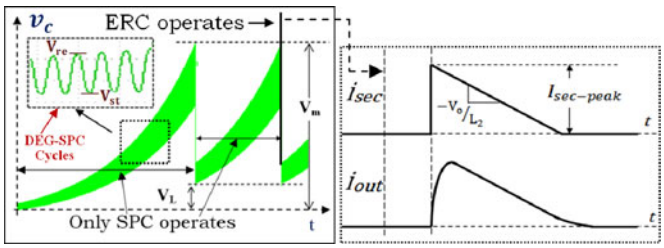

Fig. 10. DEG voltage under the influence of the electrical subsystem.

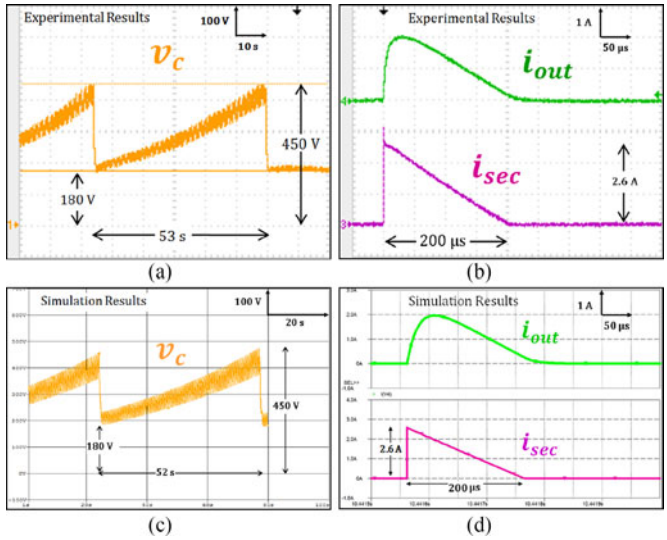

Fig. 11. Experimental waveforms of (a) DEG voltage (v_c), (b) output current, and secondary current. Simulation results of (c) DEG voltage, (d) output current, and secondary current ERC for similar DEG operating conditions.

B. Electrical Subsystem

The electrical subsystem, shown in Fig. 9, has two sections:

1) Self-priming circuit;
2) Energy recovery circuit (ERC).

The self-priming circuit [15] is used to boost up the DEG voltage from very low value (6–10 V) to hundreds of volts, without the need of a high-voltage power supply or a high-voltage transformer. The voltage across the DEG–SPC terminals increases with each cycle of DEG operation, as shown in Fig. 10. Though the SPC can boost the DEG voltage passively, it requires some charge to begin its operation. This pre-charge is supplied from V_{pc}, typically a 6-V battery. Once the precharge is done, V_{pc} is isolated from the system by operating the mechanical switch S_m.

As shown in Fig. 10, voltage waveform v_c consists of many cycles of DEG operation. The voltage ripple is the variation in DEG voltage when it is stretched and relaxed continuously. Though the voltage ripple is always present in v_c, with increase in DEG operating voltage, ripple magnitude increases. In one DEG operating cycle, voltage (v_c) varies between two voltage levels V_{re} and V_{st}. So, the voltage ripple (Δv) is given by

$$\Delta v = V_{re} - V_{st}.$$

By replacing V_{re} from (1) in the aforementioned equation, we get

$$\Delta v = KV_{st} - V_{st} = V_{st}\,(K - 1).$$

As DEG voltage gain (K) is fixed, with increase in input voltage (V_{st}), ripple in v_c also increases.

With each cycle of DEG operation, the voltage across DEG–SPC terminals (v_c) increases. During this interval ERC remains idle and only DEG–SPC operates. Once the DEG voltage reaches the predefined maximum V_m, ERC operates. With operation of ERC, the voltage across the DEG terminals reduces and the current starts flowing in the secondary of the ERC $(i_{\rm sec})$ and then into the battery $(i_{\rm out})$. This process is illustrated in Fig. 10. The charge flowing into the battery, i.e., area under the $i_{\rm out}$ curve, is directly proportional to the amount of energy harvested. The ERC is operated in such a way that voltage across the DEG terminals does not fall to zero and is limited to a predefined minimum, which is marked as V_L in Fig. 10. This is achieved by controlling the turn-on time of ERC switch and enables the DEG–SPC to operate without needing any furthur precharge.

C. Experimental Verification

A prototype DEG is made from 3M-VHB 4910 material. A complete system to drive the DEG is also designed in the laboratory. Initially, the complete energy harvesting system is operated between 180 and 450 V. Experimental waveforms of DEG voltage (v_c), current flowing in the secondary of the fly-back converter $(i_{\rm sec})$, and output current $(i_{\rm out})$ are shown in Fig. 11(a) and (b), respectively. As shown in Fig. 11(a), DEG takes 53 s to boost its voltage from 180 to 450 V, and during operation of ERC, the peak of $i_{\rm sec}$ is 2.6 A. A similar energy harvesting system is designed in Orcad PSpice software where the DEG is replaced by the proposed model. Control inputs to the model and model parameters ($C_{st} = 3.1\,{\rm nF}$, $K = 2.4$, and $f = 1.8\,{\rm Hz}$) are measured by performing experiments explained in Section IV. Results obtained from the model simulation are illustrated in Fig. 11(c) and (d). As illustrated in Fig. 11(c), DEG voltage v_c takes 52 s to boost the DEG voltage from 180 to 450 V. The peak of the secondary current obtained from simulation is 2.6 A.

Moreover, to check the behavior of the model for different DEG gain, physical DEG is operated with a gain $K = 2.75$. Fig. 12 shows the voltage buildup process (from 6 to 580 V) of

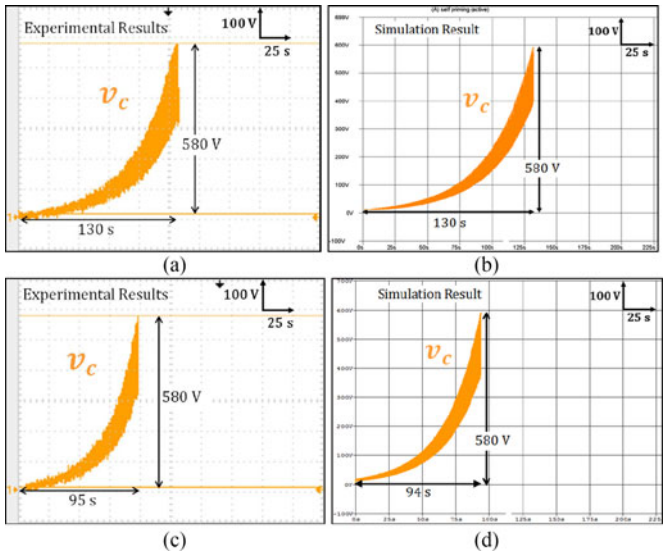

Fig. 12. Voltage buildup process of a DEG–SPC combination with $K = 2.75$. (a) Experimental and (b) simulation result with frequency $f = 2$ Hz. (c) Experimental and (d) simulation result with frequency $f = 2.25$ Hz.

DEG–SPC combination under two different DEG operating frequencies. Fig. 12(a) shows the experimentally obtained waveform of the voltage buildup process when DEG voltage gain (K) is equal to 2.75 and DEG is subjected to a mechanical vibration of 2 Hz frequency. A similar schematic is simulated in PSpice where the DEG is replaced by the proposed model. The simulation result is shown in Fig. 12(b). Similar procedure, for both experiment and simulation, is repeated by increasing the DEG operating frequency (f) to 2.25 Hz. The experimental and simulation results obtained are depicted in Fig. 12(c) and (d), respectively. It is clear from Figs. 11 and 12 that, the results obtained from the model simulation are close to the actual DEG results. The model accurately predicts the voltage buildup time and the amount of energy harvested from a physical DEG energy harvesting system.

VI. Conclusion

This letter starts with an introduction to DEG operating cycle. Based on the insights derived from the energy harvesting cycle, an electrical circuit model for the DEG is proposed. Methods to obtain different model inputs from a physical DEG are explained at length. The proposed model is simulated in PSpice simulation platform, and performance of the DEG is compared with that of an experimental prototype. Though the proposed model is simple and approximate, it reflects the electromechanical dependency in DEG and successfully imitates the DEG behavior. This model can be a useful tool in designing DEG driving circuitry and verifying their compatibility with the DEG.

Acknowledgment

The authors would like to thank Prof. S. Basu and A. Srivastava for their suggestions and continuous support.

References

[1] H. Prahlad, R. Kornbluh, R. Pelrine, S. Stanford, J. Eckerle, and S. Oh, "Polymer power: Dielectric elastomers and their applications in distributed actuation and power generation," in *Proc. ISSS*, 2005, Bangalore, India, pp. SA-100–SA-107.

[2] L. Liu, Y. Liu, and J. Leng, "Theory progress and applications of dielectric elastomers," *Int. J. Smart Nano Mater.*, vol. 4, no. 3 2013, pp. 199–209.

[3] Y. Bar-Cohen, "Biologically inspired technology using electro active polymers (EAP)," in *Proc. SPIE,* 2006, vol. 6168, p. 616803.

[4] G. Kofod *et al.*, "Energy minimization for self-organized structure formation and actuation," *Appl. Phys. Lett.* vol. 90, no. 8, p. 081916, 2007.

[5] R. Pelrine, R. D. Kornbluh, J. Eckerle, P. Jeuck, S. Oh, Q. Pei, and S. Stanford, "Dielectric elastomers: Generator mode fundamentals and applications," in *Proc. SPIE*, 2001, vol. 4329, pp. 148–56.

[6] S. Roundy, P. K. Wright, and J. M. Rabaey, *Energy Scavenging for Wireless Sensor Networks*. Boston, MA, USA: Kluwer, 2004.

[7] C. Graf, M. Aust, J. Maas, and D. Schapeler, "Simulation model for electro active polymer generators," in *Proc. 10th IEEE Int. Conf. Solid Dielectrics*, Potsdam, 2010, pp. 1–4.

[8] B. Czech, R. van Kessel, P. Bauer, and J. A. Ferreira, "Dielectric elastomers as generators," in *Proc. 2011 14th Eur. Conf. Power Electron. Appl.*, Birmingham, 2011, pp. 1–10.

[9] C. M. Hackl, H.-Y. Tang, R. D. Lorenz, L.-S. Turng, and D. Schroder, "A multidomain model of planar electro-active polymer actuators," *IEEE Trans. Ind. Appl.*, vol. 41, no. 5, pp. 1142–1148, Sep.–Oct. 2005.

[10] M. Wissler and E. Mazza, "Modeling and simulation of dielectric elastomer actuators," *Smart Mater. Struct.*, vol. 14, pp. 1396–1402, 2005.

[11] S. E. C. Ge, J. Cao, A. Liu, L. Jin, and X. Jiang, "Research on power generation of dielectric elastomer based on MATLAB," in *Proc. IEEE Int. Conf. Mechatronics Autom.*, Beijing, 2015, pp. 549–554.

[12] T. McKay *et al.*, "Realizing the potential of dielectric elastomer generators," in *Proc. SPIE Smart Struct. Materials + Nondestructive Eval. Health Monitoring. Int. Soc. Optics Photonics*, 2011, pp. 79760B–79760B.

[13] C. Jean-Mistral, T. Porter, T. Vu-Cong, S. Chesné, and A. Sylvestre, "Modelling of soft generator combining electret and dielectric elastomer," in *Proc. IEEE/ASME Int. Conf. Adv. Intell. Mechatronics*, *Besacon*, 2014, pp. 1430–1435.

[14] C. Graf and J. Maas, "Evaluation and optimization of energy harvesting cycles using dielectric elastomers," in *Proc. SPIE*, 2011, vol. 7976, p. 79760H.

[15] T. McKay, B. OBrien, E. Calius, and I. Anderson, "Self priming dielectric elastomer generators," *Smart Mater. Struct.*, vol. 19, no. 5, Apr. 9, 2010, p. 055025.